[5] Przemieniecki, J. S., "Matrix structural analysis of substructures," AIAA J. 1, 138–147 (1963).
[6] Hurty, W. C., "Vibrations of structural systems by component mode synthesis," Proc. Am. Soc. Civil Engrs., J. Eng. Mech. Div. 86, 51–69 (August 1960).
[7] Hurty, W. C., "Dynamic analysis of structural systems by component mode synthesis," Jet Propulsion Lab., California Institute of Technology TR 32-530 (January 1964).
[8] Gladwell, G. M. L., "Branch mode analysis of vibrating systems," J. Sound Vibration 1, 41–59 (1964).

APRIL 1965 AIAA JOURNAL VOL. 3, NO. 4

Liquid Surface Oscillations in Longitudinally Excited Rigid Cylindrical Containers

FRANKLIN T. DODGE,* DANIEL D. KANA,† AND H. NORMAN ABRAMSON‡
Southwest Research Institute, San Antonio, Texas

The results of a theoretical and experimental study of low-frequency liquid surface motions in a longitudinally vibrated tank are presented and discussed in some detail. Large-amplitude free surface motions occur when the liquid responds as a one-half subharmonic of the excitation. This form of response exhibits "jump" phenomena common to nonlinear systems. Harmonic and superharmonic liquid surface motions are also observed, although their amplitudes are usually smaller than those corresponding to the one-half subharmonic response. Comparison between theoretical and experimental results are given, in most instances the correlation being rather close.

Nomenclature§

$\bar{a}_{mn}(a_{mn})$	=	amplitude of the m, nth liquid surface mode
$\bar{\alpha}_{mn}(\alpha_{mn})$	=	amplitude of the m, nth component of the liquid velocity potential
d]	=	tank diameter
$h(b)$	=	liquid depth
J_m	=	mth order Bessel function of first kind
$\bar{\lambda}_{mn}(\lambda_{mn})$	=	defined by $J_m'(\lambda_{mn}R) = 0$
$N\omega$	=	tank excitation frequency (N is a positive number)
$\bar{\Phi}(\phi)$	=	liquid velocity potential
$\bar{r}, \theta, \bar{z}(r, \theta, z)$	=	tank fixed coordinate system
R	=	tank radius
σ	=	frequency parameter, ω/ω_{kl}
$\bar{t}(t)$	=	time
$\bar{u}, \bar{v}, \bar{w}$	=	fluid velocity components
$X_0(\epsilon)$	=	tank excitation amplitude
$\bar{y}(y)$	=	free surface displacement above mean level of liquid
Y_0	=	one-half the sum of the maximum liquid surface excursion in the positive and negative direction

Presented as Preprint 65-83 at the AIAA 2nd Aerospace Sciences meeting, New York, January 25–27, 1965; revision received January 11, 1965. The results presented in this paper were obtained during the course of research sponsored by the Marshall Space Flight Center of NASA under Contract No. NAS8-11045. The authors wish to express their appreciation to Dennis Scheidt for his aid in the experimental program, to the staff of the Southwest Research Institute Computations Laboratory for performing most of the numerical work, and to David DeArmond and Victor Hernandez for preparing the figures. Our thanks are also given to the referees for several valuable comments.

* Senior Research Engineer, Department of Mechanical Sciences. Associate Member AIAA.
† Senior Research Engineer, Department of Mechanical Sciences. Member AIAA.
‡ Director, Department of Mechanical Sciences. Associate Fellow Member AIAA.

§ Symbols in parenthesis are the nondimensional equivalents of the preceding quantity.

I. Introduction

THE importance of liquid sloshing on the over-all dynamics of liquid fuel rockets is well recognized, and extensive investigations of this problem have been conducted and reported. Papers given by Abramson[1] and Cooper[2] review much of this work.

Liquid sloshing can be excited by a variety of motions of the liquid container; of these, longitudinal oscillations of the vehicle and the subsequent liquid response generally have been the least investigated. This is probably a result of the fact that linear analysis, which adequately predicts resonant frequencies and liquid responses for most types of container motion, fails to predict the liquid response amplitudes for longitudinal forced motion. Some previous linear analyses and experiments, however, have yielded results that give the over-all liquid behavior, with the exception of response amplitude, and vividly describe the complexity of this problem.

A nonlinear analysis, which predicts the complete liquid response, has been performed for an infinitely deep, very narrow rectangular tank by Yarymovych and Skalak.[3] No such nonlinear analysis has been conducted previously for the circular cylindrical tank. The purpose of the present paper, therefore, is to present a comprehensive nonlinear analytical and experimental study of liquid sloshing in a longitudinally excited, finite depth, rigid, circular cylindrical tank with emphasis placed chiefly on low-frequency excitation and the corresponding liquid response.

II. Interpretation of Mathieu Stability Chart

The frequency of the liquid surface motion for most forms of forced vibration of a container usually corresponds to the excitation frequency, and the amplitude of the motion can be calculated accurately by a linear analysis. A nonlinear analysis is necessary here only when large amplitude motions occur in the vicinity of a free surface resonance. In con-

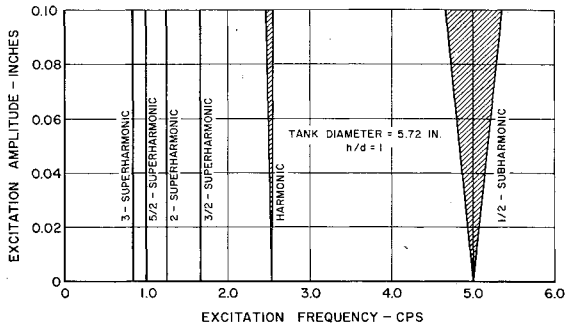

Fig. 1 Partial Mathieu stability chart for $m = 1$, $n = 1$ mode.

trast, however, the liquid surface response to longitudinal tank motion is characterized by a wide range of frequencies, most of them different from the excitation frequency. Experimentally, it has been found that the amplitude of the liquid motion becomes very large in several narrow ranges of forcing frequency, even for very small forcing amplitudes, as, for example, in the case when the exciting frequency is about twice one of the linear natural frequencies of the liquid surface; such a response is usually referred to as a "one-half subharmonic response." Existing linear analyses predict only the onset of this liquid motion, because it is found that in this case even small amplitude liquid surface motions are unstable for reasons similar to those pointed out by Taylor.[4] Among others, Bolotin,[5] Benjamin and Ursell,[6] Skalak and Yarymovych,[3] and Skalak and Conly[7] have shown that the small amplitude liquid oscillations are described by a linear differential equation with periodic coefficients, which becomes the Mathieu equation when the excitation is harmonic.[8–10]

Liquid responses for other than subharmonic motions are usually quite small but some confusion about them is evident in the published literature; for example, some authors state that the liquid response is zero except in the subharmonic frequency ranges.[7] However, for sufficiently large forcing amplitudes, large-amplitude liquid motions originating as *unstable* small motions may occur for which the predominant frequency is not a subharmonic. Also, Stoker[9] recognizes that there exist *stable* solutions of Mathieu's equation that can be any order of subharmonic or superharmonic, even though these responses will probably be severely attenuated by damping in an actual physical system. It appears that most of the aforementioned confusion is caused by misinterpreting the Mathieu stability chart. For this reason, a rather detailed description of the possible types of liquid motions is given in this section of the present paper.

Benjamin and Ursell[6] and others have shown that the small motions of an ideal liquid in a vertically vibrated tank are described by Mathieu's equation in the form

$$\frac{d^2\bar{a}_{mn}}{d\bar{t}^2} + \left(\omega_{mn}{}^2 - \omega_{mn}{}^2 \frac{\omega^2 X_0}{g}\cos\omega\bar{t}\right)\bar{a}_{mn} = 0 \qquad (1)$$

where ω_{mn} is one of the natural frequencies of free liquid sloshing¶; $\bar{a}_{mn}$ is the amplitude of the corresponding mode of the liquid surface motion, measured relative to the moving tank; ω is the forcing frequency; g is the acceleration due to gravity (or any other uniform longitudinal acceleration to which the tank is subjected); and X_0 is the amplitude of the tank motion. Solutions of this equation can be either stable or unstable[8]: that is, $\bar{a}_{mn}$ can either remain bounded in magnitude or else grow large without limit. In both cases, however, Eq. (1) does not predict the amplitude of the sloshing $\bar{a}_{mn}$ since any solution of (1) can be multiplied by a constant factor and still satisfy (1). Consequently, since Eq. (1) was derived by using the classical theory of potential flow with linearized boundary conditions at the free surface, a nonlinear analysis must be used to calculate the amplitude of even relatively small liquid motions.**

The regimes of stable and unstable solutions of Eq. (1) are usually shown in a Mathieu stability chart. Such charts are generally presented in terms of dimensionless variables, but a much clearer picture of the type of possible liquid motions for any given tank size and liquid depth can be obtained from a dimensional plot. Figure 1 shows such a stability diagram for a tank with a diameter of 5.72 in. (the tank used in most of our experiments) and a liquid depth equal to the tank diameter. Only a few of the stable and unstable regions corresponding to the sloshing mode of lowest natural frequency, the $m = 1$, $n = 1$ antisymmetrical mode, are shown in this diagram, with the regions of unstable solutions of (1) shown as shaded. This chart was constructed from the standard nondimensional forms by employing the appropriate formulas given by Stoker[9] and the results of Benjamin and Ursell.[6]

The unshaded, stable regions in Fig. 1 are interconnected at the points $X_0 = 0$, $\omega = (2/k)\omega_{mn}$ for k an integer; at these points, the solutions to Eq. (1) are either $\cos(k/2)\omega t$ or $\sin(k/2)\omega t$, both of which correspond to free oscillations of the liquid surface. If the amplitude of the tank motion X_0 and the magnitude of the forcing frequency ω are such that the point (ω, X_0) falls in the shaded region farthest to the right in Fig. 1, the small liquid motions predominantly of the form $\cos\frac{1}{2}\omega t$ (or $\sin\frac{1}{2}\omega t$) are unstable, and a large-amplitude free surface motion is produced.†† If ω and X_0 are such that $k = 2$, small motions of the form $\cos\omega t$, i.e., harmonic motions, are unstable, and a large amplitude motion with the same period as the tank motion is eventually obtained. For other values of k, unstable motions of the form $\cos\frac{3}{2}\omega t$, $\cos 2\omega t$, $\cos\frac{5}{2}\omega t$, . . . , occur, so that it is possible, at least theoretically, to obtain large amplitude superharmonic motion of all orders.‡‡

The unstable regions shown in Fig. 1 are based upon the assumption of an inviscid fluid; with any real fluid, the unstable regions are slightly narrower than shown and do not extend completely to the line $X_0 = 0$. Since the $\frac{1}{2}$-subharmonic region is the widest of the unstable regions, it exhibits the smallest amplitude cutoff; the other unstable regions, which are very narrow, usually are not present at all except for prohibitively large values of the forcing amplitude or unless the tank diameter is very small.§§ Consequently, the one-half subharmonic is the only large amplitude periodic liquid motion that is normally observed experimentally. However, there is a possibility that small-amplitude liquid motions, which do not grow from unstable motions, can occur in the neighborhood of other unstable regions; in fact, such harmonic and double superharmonic liquid motions have been observed in the experiments described in this report.

¶ For a circular cylindrical tank,

$$\omega_{mn}{}^2 = \left[\left(\frac{2\xi_{mn}}{d}\right)^3 \frac{\gamma}{\rho} + \frac{2\xi_{mn}g}{d}\right]\tanh\frac{2\xi_{mn}h}{d}$$

where d is the tank diameter, γ is the liquid surface tension, ρ is the liquid density, and ξ_{mn} are the roots of $J_m'(\xi_{mn}) = 0$.

** This statement is true only for the unstable solutions of Eq. (1). The stable, small-amplitude liquid motions can be calculated from Eq. (1), as was pointed out by one of the referees.

†† It should be noted that the liquid motion that eventually results is not a pure $\cos\frac{1}{2}\omega t$ (or $\sin\frac{1}{2}\omega t$) form since it also contains components oscillating at other frequencies as well. The motion is, however, periodic with a period equal to twice the period of the exciting motion.

‡‡ Figure 1 shows only the unstable regions for $k \leqslant 6$.

§§ The width of the unstable regions increases with decreasing tank diameter.

Figure 1 also indicates that the only subharmonic liquid motion that occurs as a result of an instability in small liquid motions is the one-half subharmonic, contrary to previous assertions of some other investigators. It is possible that higher-order subharmonics, e.g., the $\frac{1}{4}$-subharmonic, may occur, but these are not the result of the same kind of instabilities that give rise to the $\frac{1}{2}$-subharmonic motion.

Actually, the Mathieu diagram for any given tank and liquid depth is much more complicated even than that indicated in Fig. 1. The unstable regions for several $\frac{1}{2}$-subharmonic modes, and the locations of several linear free modes in the same frequency range, are shown in Fig. 2. From this chart, one can see that the unstable regions for various sloshing modes overlap considerably, and it is apparent that this overlapping of regions becomes even more congested as the frequency is increased. It can be seen, however, from Fig. 2 that the first antisymmetrical and first symmetrical modes can be fairly well isolated, at least for small values of X_0, so that they are convenient modes to study both experimentally and analytically.

It should be carefully borne in mind that, in a dimensionless Mathieu diagram, all of the $\frac{1}{2}$-subharmonic regions shown in Fig. 2 are compressed into one region, with the result that it is difficult to foresee the degree of overlapping of the various modes. Likewise, all of the other kinds of unstable regions are compressed into separate regions, one region for the harmonic response, one for the double superharmonic response, and so on. Thus, for a given tank, the dimensional stability chart describes much more vividly the liquid behavior predicted by the Mathieu equation.

III. Theoretical Analysis

A. Basic Equations

The wave motion theory developed in this section is valid only for low-frequency tank vibrations for which the tank may be assumed to behave as a rigid container, and capillary or surface-tension effects on the liquid surface waves have been neglected. The fluid is assumed to be inviscid and its motion irrotational; both assumptions are justified by past experimental work in sloshing. The aim of the analysis is to predict the amplitudes of the liquid free surface motions, the corresponding wave shapes, and the frequency bands for which such motions are possible. The general method of attack is similar to that used by Skalak and Yarymovych[3] and Penney and Price.[11]

Figure 3 shows the liquid-tank geometry. A cylindrical coordinate system is fixed at the mean level of the liquid; thus, it has the same motion as the base of the tank, which is given by $X = X_0 \cos N\omega\bar{t}$. If the frequency of the predominant liquid motion is given by ω, then allowing N to assume various positive values specifies whether or not the predominant liquid response is subharmonic, harmonic, or superharmonic.

The fluid velocity components ($\bar{u}$, $\bar{v}$, $\bar{w}$ in the $\bar{r}$, θ, and $\bar{z}$ directions of the moving coordinate system) may be obtained from a potential $\bar{\phi}$, which satisfies Laplace's equation,

$$\frac{\partial^2\bar{\phi}}{\partial\bar{r}^2} + \frac{1}{\bar{r}}\frac{\partial\bar{\phi}}{\partial\bar{r}} + \frac{1}{\bar{r}^2}\frac{\partial^2\bar{\phi}}{\partial\theta^2} + \frac{\partial^2\bar{\phi}}{\partial\bar{z}^2} = 0 \qquad (2)$$

The velocity components are

$$\bar{u} = -\frac{\partial\bar{\phi}}{\partial\bar{r}} \qquad \bar{v} = -\frac{\partial\bar{\phi}}{\bar{r}\partial\theta} \qquad \bar{w} = -\frac{\partial\bar{\phi}}{\partial\bar{z}} \qquad (3)$$

and the fluid velocity normal to the tank walls and bottom must be zero. Consequently,

$$\partial\bar{\phi}/\partial\bar{r} = 0 \text{ at } \bar{r} = R \qquad (4)$$

$$\partial\bar{\phi}/\partial\bar{z} = 0 \text{ at } \bar{z} = -h \qquad (5)$$

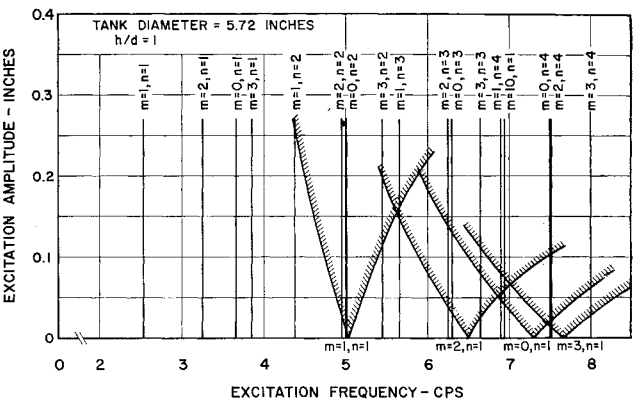

Fig. 2 General liquid behavior below 8 cps.

The solution of Eq. (2) which also satisfies (4) and (5) is

$$\bar{\phi} = \bar{\alpha}_o + \sum_{m=0}^{\infty}\sum_{n=1}^{\infty} \bar{\alpha}_{mn} J_m(\bar{\lambda}_{mn}\bar{r}) \cos m\theta \frac{\cosh\bar{\lambda}_{mn}(\bar{z}+h)}{\cosh\bar{\lambda}_{mn}\bar{h}} \qquad (6)$$

$J_m(\bar{\lambda}_{mn}\bar{r})$ is the mth order Bessel function of the first kind, and $\bar{\lambda}_{mn}$ is the nth root of the equation

$$dJ_m(\bar{\lambda}_{mn}R)/d\bar{r} = 0 \qquad (7)$$

$\bar{\alpha}_o$ and all the $\bar{\alpha}_{mn}$ are as yet undetermined functions of time.¶¶ They must be chosen in such a way as to satisfy the free surface boundary conditions, one of which is that the pressure at the free surface must be constant. This may be expressed analytically by setting the surface pressure equal to the ullage pressure in Bernoulli's equation:

$$\left.\frac{\partial\bar{\phi}}{\partial\bar{t}}\right|_{\bar{z}=\bar{y}} - (g - N^2\omega^2 X_0 \cos N\omega\bar{t})\bar{y} - \frac{1}{2}\left[\left(\frac{\partial\bar{\phi}}{\partial\bar{r}}\right)^2 + \left(\frac{\partial\bar{\phi}}{\bar{r}\partial\theta}\right)^2 + \left(\frac{\partial\bar{\phi}}{\partial\bar{z}}\right)^2\right]_{\bar{z}=\bar{y}} = 0 \qquad (8)$$

where $\bar{y}$ is the displacement of the free surface above its average position, $\bar{z} = 0$.

Suppose $\eta(\bar{r}, \theta, \bar{z}, \bar{t})$ is the geometrical equation of the free surface. Then $\bar{\eta} = \bar{z} - \bar{y}(\bar{r}, \theta, \bar{t}) = 0$, and, since no fluid

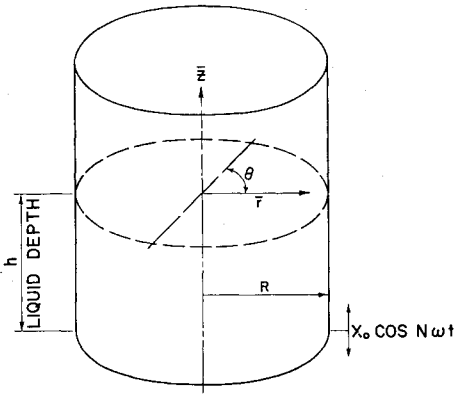

Fig. 3 Cylindrical tank and coordinate system.

¶¶ Of course, in a perfectly symmetric tank and for perfectly vertical excitation, only symmetrical sloshing is possible so that $m = 0$ in Eq. (6). But, in any real tank, slight imperfections in the geometry or the excitation admit the possibility of antisymmetrical sloshing. The line $\theta = 0$ is determined by these imperfections and so is not prescribed by the idealized theory developed here.

can cross the free surface, the kinematic boundary condition at the free surface is[12]

$$\frac{D\bar{\eta}}{D\bar{t}} = 0 \text{ or } \frac{\partial\bar{y}}{\partial\bar{t}} = \frac{\partial\bar{\phi}}{\partial\bar{r}}\frac{\partial\bar{y}}{\partial\bar{r}} + \frac{1}{\bar{r}^2}\frac{\partial\bar{\phi}}{\partial\theta}\frac{\partial y}{\partial\theta} - \frac{\partial\bar{\phi}}{\partial\bar{z}} \text{ at } \bar{z} = \bar{y} \quad (9)$$

At least in theory, the kinematic condition (9) can be solved for $\bar{y}$ in terms of $\bar{\phi}$; this solution can then be used in the pressure boundary condition (8) to give an equation in $\bar{\phi}$ only and consequently to determine the $\bar{\alpha}_{mn}$. Hence, the velocity potential can be completely determined and the liquid response and wave shape calculated. However, instead of proceeding along these lines, another method more amenable to approximate solutions is developed.

In analogy with Eq. (6), it is assumed that $\bar{y}$ may be expressed as

$$\bar{y} = \sum_{m=0}^{\infty}\sum_{n=1}^{\infty} \bar{a}_{mn}J_m(\bar{\lambda}_{mn}\bar{r})\cos m\theta \quad (10)$$

where the $\bar{a}_{mn}$ are unknown functions of time.* The boundary conditions (8) and (9) together can now be used to fix the values of $\bar{a}_{mn}$ and $\bar{\alpha}_{mn}$.

It is convenient at this point to introduce a set of dimensionless variables. Suppose that the sloshing mode under consideration grows from the k, lth free (linear) mode so that it is reasonable to assume that $\bar{\alpha}_{kl}$ and $\bar{a}_{kl}$ are the predominant amplitudes in the series expansions of $\bar{\phi}$ and $\bar{y}$. It is then appropriate to nondimensionalize the variables by using the natural frequency and a characteristic length parameter of the corresponding free motion. Thus, let

$$\sigma = \frac{\omega}{\omega_{kl}} \quad \text{where} \quad \omega_{kl} = (\bar{\lambda}_{kl}g\tanh\bar{\lambda}_{kl}h)^{1/2}$$

$$t = \omega_{kl}\bar{t} \qquad r = (\bar{\lambda}_{kl}\tanh\bar{\lambda}_{kl}h)\bar{r}$$

$$z = (\bar{\lambda}_{kl}\tanh\bar{\lambda}_{kl}h)\bar{z} \qquad a_{mn} = (\bar{\lambda}_{kl}\tanh\bar{\lambda}_{kl}h)\bar{a}_{mn}$$

$$y = (\bar{\lambda}_{kl}\tanh\bar{\lambda}_{kl}h)\bar{y} \qquad \alpha_{mn} = \frac{(\bar{\lambda}_{kl}\tanh\bar{\lambda}_{kl}h)^2}{\omega_{kl}}\bar{\alpha}_{mn}$$

$$\phi = \frac{(\bar{\lambda}_{kl}\tanh\bar{\lambda}_{kl}h)^2}{\omega_{kl}}\bar{\phi} \qquad \lambda_{mn} = \frac{\bar{\lambda}_{mn}}{\bar{\lambda}_{kl}\tanh\bar{\lambda}_{kl}h}$$

$$\epsilon = (\bar{\lambda}_{kl}\tanh\bar{\lambda}_{kl}h)X_0 \qquad b = (\bar{\lambda}_{kl}\tanh\bar{\lambda}_{kl}h)h$$

Substituting these dimensionless variables into the boundary conditions, and at the same time expanding $\cosh\lambda_{mn}(y + b)$ in Eq. (6) into a power series, allows Eq. (8), the boundary condition on pressure, to be written as

$$\dot{\alpha}_0 + \sum_{m=0}^{\infty}\sum_{n=1}^{\infty}\{[\dot{\alpha}_{mn}F^r_{mn} - (1 - N^2\sigma^2\epsilon\cos N\sigma t)a_{mn}]J_m(\lambda_{mn}r)\cos m\theta\} -$$

$$\frac{1}{2}\sum_{m=0}^{\infty}\sum_{n=1}^{\infty}\sum_{p=0}^{\infty}\sum_{q=1}^{\infty}\{\alpha_{mn}\alpha_{pq}\lambda_{mn}\lambda_{pq}J_{m+1}(\lambda_{mn}r)J_{p+1}(\lambda_{pq}r)\times$$

$$\cos m\theta\cos p\theta F^r_{mn}F_{pq}{}^s + \alpha_{mn}\alpha_{pq}\frac{mp}{r^2}J_m(\lambda_{mn}r)J_p(\lambda_{pq}r)\times$$

$$\cos(m - p)\theta F^r_{mn}F_{pq}{}^s + \alpha_{mn}\alpha_{pq}\lambda_{mn}\lambda_{pq}J_m(\lambda_{mn}r)J_p(\lambda_{pq}r)\times$$

$$\cos m\theta\cos p\theta G^r_{mn}G_{pq}{}^s - 2\alpha_{mn}\alpha_{pq}\frac{p\lambda_{mn}}{r}J_{m+1}(\lambda_{mn}r)J_p(\lambda_{pq}r)\times$$

$$\cos m\theta\cos p\theta F^r_{mn}F_{pq}\} = 0 \quad (11)$$

where the dots indicate differentiation with respect to time and

$$F^{\mu}_{\alpha\beta} = \frac{\cosh\lambda_{\alpha\beta}(y + b)}{\cosh\lambda_{\alpha\beta}b} = \sum_{\mu=0}^{\infty}\left\{\frac{\lambda^{2\mu}_{\alpha\beta}y^{2\mu}}{(2\mu)!} + \mu\frac{\lambda^{2\mu+1}_{\alpha\beta}y^{2\mu+1}}{(2\mu+1)!}\tanh\lambda_{\alpha\beta}b\right\} \quad (12)$$

$$G^{\mu}_{\alpha\beta} = \frac{\sinh\lambda_{\alpha\beta}(y + b)}{\cosh\lambda_{\alpha\beta}b} = \sum_{\mu=0}^{\infty}\left\{\frac{\lambda^{2\mu}_{\alpha\beta}y^{2\mu}}{(2\mu)!}\tanh\lambda_{\alpha\beta}b + \frac{\lambda^{2\mu+1}_{\alpha\beta}y^{2\mu+1}}{(2\mu+1)!}\right\} \quad (13)$$

and

$$y = \sum_{m=0}^{\infty}\sum_{n=1}^{\infty} a_{mn}J_m(\lambda_{mn}r)\cos m\theta$$

The kinematic boundary condition, Eq. (9), can be written as

$$\sum_{m=0}^{\infty}\sum_{n=1}^{\infty}\{[\dot{a}_{mn} + \lambda_{mn}\alpha_{mn}G^r_{mn}]J_m(\lambda_{mn}r)\cos m\theta\} =$$

$$\sum_{m=0}^{\infty}\sum_{n=1}^{\infty}\sum_{p=0}^{\infty}\sum_{a=1}^{\infty}\{\alpha_{mn}a_{pq}\lambda_{mn}\lambda_{pq}J_{m+1}(\lambda_{mn}r)J_{p+1}(\lambda_{pq}r)\times$$

$$\cos m\theta\cos p\theta F^r_{mn} + \alpha_{mn}a_{pq}\frac{mp}{r^2}J_m(\lambda_{mn}r)J_p(\lambda_{pq}r)\times$$

$$\cos(m - p)\theta F_{mn} - \alpha_{mn}a_{pq}\frac{m\lambda_{pq}}{r}J_m(\lambda_{mn}r)J_{p+1}(\lambda_{pq}r)\times$$

$$\cos m\theta\cos p\theta F^r_{mn} - \alpha_{mn}a_{pq}\frac{p\lambda_{mn}}{r}J_{m+1}(\lambda_{mn}r)J_p(\lambda_{pq}r)\times$$

$$\cos m\theta\cos p\theta F^r_{mn}\} \quad (14)$$

Equations (11) and (14) can now be solved approximately to give the values of the α_{mn} or a_{mn} for various special cases. The first general type of liquid motion investigated here is the one-half subharmonic response, for which $N = 2$ in Eq. (11); the response can be further subdivided into antisymmetrical and symmetrical sloshing.

B. Antisymmetrical One-Half Subharmonic Sloshing

Only the first, lowest frequency, antisymmetrical sloshing mode is considered here, but the same general method can be applied to other modes as well. For this case, α_{11} and a_{11} are the predominant amplitudes so that the appropriate k and l used to nondimensionalize the variables must be $k = l = 1$.

Obviously, only a finite number of terms in Eqs. (11) and (14) can be retained if there is to be any possibility of obtaining even an approximate solution of the equations. Because of the previous analytical study of rectangular tanks,[3] it appears that terms at least up to the third order in the dominant amplitudes must be retained. Observation of the experimental surface waves showed that a symmetrical wave and a $\cos 2\theta$ wave were superimposed on the fundamental $\cos\theta$ antisymmetrical wave, but one can also demonstrate analytically that the first symmetrical mode and the first $\cos 2\theta$ mode are the largest of the small amplitude waves superimposed on the basic $\cos\theta$ mode. In order to do this, Eqs. (11) and (14) are considered as functions of θ and r, and these functions are then expanded in a Fourier series of $\cos m\theta$ terms, $m = 0, 1, 2, \ldots$. By collecting terms that are independent of θ but which vary with r in each of the resulting series, and noting that both infinite series must equal zero for all values of θ and r, so that the coefficient of each cosine must be identically zero, it can be seen that the sum (over n) of all the terms that vary linearly with a_{0n} or α_{0n} must equal the sum of such nonlinear terms as $a_{1n}\alpha_{1n}$, $a_{2n}\alpha_{2n}$, $\alpha_{1n}{}^2$, . . . , and terms to the fourth power or higher in the other amplitudes.†

* The constant term in Eq. (10), say $\bar{a}_0$, is zero since the average value of $\bar{y}$ over the tank surface must be zero.

† Collecting terms that are independent of both θ and r gives an equation that specifies α_0 in terms of the other α_{mn} and a_{mn}. But α_0 determines the arbitrary additional function of time in the velocity potential and is only needed when calculating the pressure.

By collecting terms that vary as $\cos 2\theta$, it can be seen that the sum of all the terms that vary linearly with a_{2n} or α_{2n} must equal the sum of such nonlinear terms as $a_{1n}\alpha_{1n}$, $a_{2n}\alpha_{2n}$, α_{1n}^2, . . . , and terms to the fourth power or higher in the other amplitudes.

By collecting terms that vary as $\cos\theta$ it can be seen that the sum of all the terms that vary linearly with α_{1n} or a_{1n} must equal the sum of such terms as $a_{1n}^2\alpha_{1n}$, $a_{1n}\alpha_{1n}^2$, α_{1n}^3, $a_{1n}\alpha_{0n}$, $\alpha_{1n}a_{2n}$, . . . , and terms to the fifth power or higher in α_{1n} or a_{1n}, or the second power or higher in a_{2n}, α_{2n}, a_{0n}, and α_{0n}. But, by hypothesis, a_{11} and α_{11} are the dominant amplitudes; thus, for $n \neq 1$, a_{1n} or α_{1n} can be no larger in amplitude than about a_{11}^3, or, in other words, they are at least third-order terms. Hence, with an accuracy correct to the third order, the sum of the terms linear in a_{0n} and α_{0n}, or linear in a_{2n} and α_{2n}, depends only on a_{11}^2, α_{11}^2, and $a_{11}\alpha_{11}$, according to the previous two paragraphs.

Now, by expanding the group of terms that are independent of θ, but which vary with r, in a Bessel series of $J_0(\lambda_{0n}r)$ terms (such terms correspond to symmetrical sloshing modes), one can see that a_{01} or α_{01} is much larger than any other a_{0n} or α_{0n}. In fact, a_{01} is about ten times as large as the sum of the rest of the a_{0n}, so that only a_{01} or α_{01} need be retained. The result of these manipulations is that the part of Eq. (11) that is independent of θ, and correct to the third order in a_{11} and α_{11}, may be written as‡

$$[\dot{\alpha}_{01} - (1 - 4\sigma^2\epsilon\cos 2\sigma t)a_{01} - 0.121482\dot{a}_{11}a_{11} - \alpha_{11}^2(0.070796\lambda_{11}^2 - 0.060741)]J_0(\lambda_{01}r) = 0 \quad (15)$$

and the corresponding part of (14) is

$$[\dot{a}_{01} + \alpha_{01}\lambda_{01}\tanh\lambda_{01}b - 0.263074\lambda_{11}^2\alpha_{11}a_{11}]J_0(\lambda_{01}r) = 0 \quad (16)$$

A similar procedure for the parts of (11) and (14) that vary as $\cos 2\theta$ or $\cos\theta$, i.e., expanding them in a Bessel series of $J_2(\lambda_{2n}r)$ terms, or $J_1(\lambda_{1n}r)$ terms, respectively, leads to similar but somewhat more lengthy expressions.§

However, for a linear analysis, Eqs. (11) and (14) reduce to

$$\dot{\alpha}_{11} - (1 - 4\sigma^2\epsilon\cos 2\sigma t)a_{11} = 0$$

$$\dot{a}_{11} + \alpha_{11} = 0$$

which can be combined to give one equation in the liquid free surface amplitude

$$\ddot{a}_{11} + (1 - 4\sigma^2\epsilon\cos 2\sigma t)a_{11} = 0 \quad (17)$$

Equation (17) is a dimensionless form of Eq. (1) for the special case of one-half subharmonic liquid motion.

The approximate range of unstable solutions of Eq. (17) can be found by assuming that a_{11} is adequately represented by

$$a_{11} = A\sin\sigma t + B\cos\sigma t$$

in which a subharmonic motion is assumed since the frequency of the motion is written as one-half the exciting frequency. Substituting this solution into Eq. (17) and collecting the coefficients of $\sin\sigma t$ and $\cos\sigma t$ shows that either

$$A \neq 0 \qquad B = 0 \qquad \sigma^2 = 1/(1 - 2\epsilon) \quad (18)$$

or else

$$A = 0 \qquad B \neq 0 \qquad \sigma^2 = 1/(1 + 2\epsilon) \quad (19)$$

Hence, according to the general theory of Mathieu's equation, for σ^2 in the range $1/(1 + 2\epsilon) \leqslant \sigma^2 \leqslant 1/(1 - 2\epsilon)$, the value of a_{11} grows exponentially in time. Thus, in this range of σ, small liquid motions are unstable; this range of σ, moreover, agrees with the results of Stoker[9] discussed in the preceding section of this paper.

If $\epsilon = 0$, the value of σ is unity, which, in dimensional terms, implies that the free surface oscillates with a frequency equal to ω_{11}, the natural frequency of free oscillations.

In order to determine the amplitude of the sloshing, the complete set of nonlinear equations must be solved. It should be noted that, if the equations are simplified by keeping only terms up to the second order, a_{11} would still not be determined since the equations leading to (17) do not contain any second-order terms.

Because the amplitude of the free surface motion, and not the velocity potential itself, is most easily correlated with experimental data, the set of nonlinear equations¶ is combined by retaining only terms up to the third order to give three second-order ordinary differential equations in the three time-varying amplitudes a_{11}, a_{01}, and a_{21}. The results are

$$\ddot{a}_{11} + (1 - 4\sigma^2\epsilon\cos 2\sigma t)a_{11}(1 + K_{11}a_{11}^2 + K_{01}a_{01} - K_{21}a_{21}) + 0.034780\lambda_{11}^2\ddot{a}_{11}a_{11}^2 + k_{11}\dot{a}_{11}^2a_{11} + 0.165118\ddot{a}_{01}a_{11} - 0.198686\ddot{a}_{21}a_{11} + k_{01}\dot{a}_{01}\dot{a}_{11} - k_{21}\dot{a}_{21}\dot{a}_{11} = 0 \quad (20)$$

$$\ddot{a}_{01} + \lambda_{01}\tanh\lambda_{01}b(1 - 4\sigma^2\epsilon\cos 2\sigma t)a_{01} - \ddot{a}_{11}a_{11}(0.121482\lambda_{01}\tanh\lambda_{01}b - 0.263074\lambda_{11}^2) + \dot{a}_{11}^2[\lambda_{01}^2\tanh\lambda_{01}b(0.070796\lambda_{11}^2 - 0.060741) + 0.263074\lambda_{11}^2] = 0 \quad (21)$$

$$\ddot{a}_{21} + \lambda_{21}\tanh\lambda_{21}b(1 - 4\sigma^2\epsilon\cos 2\sigma t)a_{21} + \ddot{a}_{11}a_{11}(0.350807\lambda_{21}\tanh\lambda_{21}b - 0.482670\lambda_{11}^2) + \dot{a}_{11}^2[\lambda_{21}\tanh\lambda_{21}b(0.175403 - 0.065931\lambda_{11}^2) - 0.482670\lambda_{11}^2] = 0 \quad (22)$$

The rather lengthy constants in Eq. (20) are given in the Appendix.

A complete third-order theory would include the determination of a few other a_{mn} that are about of the magnitude of a_{11}^3. However, these a_{mn} are not needed to determine any of a_{11}, a_{01}, or a_{21} and hence are not given here. At any rate, such terms are at least one order of magnitude smaller than a_{01} or a_{21}, and two orders smaller than a_{11}.

Equations (20), (21), and (22) are satisfied to within the accuracy of third-order terms by either of two sets of solutions, both chosen in analogy with the two independent solutions of the linear equation (17). Thus, either

$$a_{11} = A\sin\sigma t + A_{13}^3\sin 3\sigma t$$

$$a_{01} = A_{00}^2 + A_{02}^2\cos 2\sigma t$$

$$a_{21} = A_{20}^2 + A_{22}^2\cos 2\sigma t \quad (23)$$

or

$$a_{11} = B\cos\sigma t + B_{13}^3\cos 3\sigma t$$

$$a_{01} = B_{00}^2 + B_{02}^2\cos 2\sigma t$$

$$a_{21} = B_{20}^2 + B_{22}^2\cos 2\sigma t \quad (24)$$

The superscripts on the A_{ij} and B_{ij} indicate their order of magnitude in comparison to A or B, e.g., A_{00}^2 is about the magnitude of $(A)(A) = A^2$.

All of the A_{ij} and B_{ij} may be calculated by substituting one or the other of these sets of solutions (23) or (24) into the set of differential equations (20), (21), and (22) and then equating coefficients of the constant terms, $\sin\sigma t$ terms, $\cos\sigma t$ terms, $\cos 2\sigma t$ terms, $\sin 3\sigma t$ terms, and $\cos 3\sigma t$ terms.

‡ Because some of the integrals in the Bessel series expansions were evaluated numerically, the resulting equations may not be as accurate as the six decimal places that were retained in the coefficients of the nonlinear terms might indicate.

§ Space limitations preclude the inclusion of many of the details of this analysis. The more important equations and some numerics are given in Ref. 19.

¶ Equations (15) and (16) and their counterparts (not given explicitly in this paper).

The resulting expressions for the A_{ij} are quite lengthy and are given in detail in Ref. 19.

Results for the alternate solution (24) are similar to those given by (23), but a different relation between the sloshing amplitude and the parameters σ and ϵ is predicted. Only the amplitude-frequency relation given by (23), however, is observed experimentally. Hence, (24) must be an unstable approximate solution to the set of differential equations; this can be demonstrated analytically by the method of Andronow and Witt,[9] as shown in Ref. 19.

By collecting the preceding results, the dimensionless sloshing amplitude may be written as

$$y = (A \sin\sigma t + A_{13}^3 \sin 3\sigma t) J_1(\lambda_{11} r) \cos\theta + (A_{00}^2 + A_{02}^2 \cos 2\sigma t) J_0(\lambda_{01} r) + (A_{20}^2 + A_{22}^2 \cos 2\sigma t) J_2(\lambda_{21} r) \cos 2\theta \quad (25)$$

The liquid amplitude at any time and at any position, as well as the standing wave shape, may be calculated from this formula.

C. Symmetrical One-Half Subharmonic Sloshing

If in the definition of ϕ and y all terms that vary with θ are discarded, the case of symmetrical sloshing may be investigated. The appropriate values of k and l to nondimensionalize the variables, for the lowest-frequency symmetrical mode, are $k = 0$, $l = 1$. Then by linearizing the resulting equations, as before, one finds that the dominant term in the free surface series expansion a_{01} is given by

$$\ddot{a}_{01} + (1 - 4\sigma^2\epsilon \cos 2\sigma t) a_{01} = 0 \quad (26)$$

This is the same as Eq. (17) and has the same solution. As before, if definite information is desired about the magnitude of the sloshing, the equations cannot be completely linearized.

In contrast to antisymmetric sloshing, the differential equations giving the dominant amplitude contain second-order terms as well as third-order terms. Even so, the second-order terms alone do not predict the magnitude of a_{01}, and the third-order terms must be retained. As before, one of the two forms of solution is unstable and is not observed in practice. All of the A_{ij} in the stable solution may be calculated by substituting the solution into the set of differential equations and then collecting coefficients of the various harmonics. Thus, the approximate sloshing amplitude may be written as

$$y = (A \sin\sigma t + A_{10}^2 + A_{12}^2 \cos 2\sigma t + A_{13}^3 \cos 3\sigma t) J_0(\lambda_{01} r) + (A_{20}^2 + A_{22}^2 \cos 2\sigma t) J_0(\lambda_{02} r) \quad (27)$$

From this equation, the wave shape and the free surface amplitude at any time and position may be calculated.

In passing, it should be noted that the accuracy of the predicted value of the liquid sloshing amplitude for either symmetrical or antisymmetrical responses can be improved by retaining fifth- or even higher-order terms. A fourth-order theory would not improve the accuracy, but would merely refine the standing wave shape, because only terms proportional to odd powers of the a_{ij} can serve to increase the accuracy of the calculated value of the dominant amplitude.

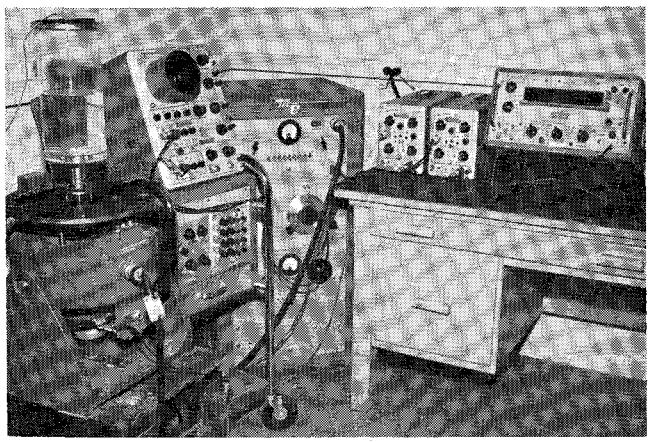

Fig. 4 Experimental apparatus.

D. Harmonic and Superharmonic Sloshing

Harmonic and superharmonic sloshing, which are also observed experimentally, can be analyzed by letting N assume the values one and one-half, respectively. Since the analysis leading up to Eqs. (20), (21), and (22) is independent of the value of N, these nonlinear equations should also be valid for antisymmetrical harmonic and superharmonic sloshing. Similar equations would hold for symmetrical sloshing.

By linearizing the set of such equations, the first antisymmetric double superharmonic sloshing mode, as an example, should be described by

$$\ddot{a}_{11} + (1 - \tfrac{1}{4}\sigma^2\epsilon \cos\tfrac{1}{2}\sigma t) a_{11} = 0 \quad (28)$$

where the frequency of the liquid motion is still denoted by σ. Employing an analysis similar to that used for the subharmonic motion gives results describing the large-amplitude double superharmonic response that grows from unstable small motion. However, such a response is usually observed only in tanks of very small diameter; for larger diameter tanks, this superharmonic response is generally a stable small-amplitude motion. The stable Mathieu function solution of Eq. (28), however, does not in general have a period exactly one-half the exciting period, and, moreover, this solution decays to zero in time if a small damping term is added to Eq. (28). Hence, it does not seem that this type of solution corresponds to the stable small amplitude harmonic and superharmonic responses. More theoretical work is needed before the small-amplitude solutions that occur in the stable regions of the Mathieu diagram are put into a satisfactory state of agreement with experiments.

IV. Experimental Apparatus

A photograph of the experimental apparatus used in the present study is shown in Fig. 4. Most of the tests were conducted in a 12-in.-long, 5.72-in.-diam tank, with a $\frac{1}{8}$-in.-thick wall, made of transparent acrylic plastic, although a few tests were run with a 3-in.-diam plastic tank. Water was used as the test liquid. The tank walls and bottom are essentially rigid in the 0- to 60-cps frequency range used for the observations. The tank is mounted on an electrodynamic shaker, which provides the longitudinal excitation. The tank mounting is designed to allow motion only along its longitudinal axis, and lateral tilting of the tank is prevented.

A liquid surface displacement transducer similar to one employed by us in previous work[13] is mounted to a fixture on the top of the tank, and includes a stiff probe that extends into the water in the tank. Essentially, it gives a measure of the length of the liquid conductance path in contact with the transducer probe. The probe contains two separated conductors that parallel part of the resistance in one of the arms of a 150-ohm Wheatstone resistance bridge. Ordinary tap water was found to be a sufficiently sensitive electrolyte to allow liquid surface displacement monitoring in the entire range of observation. The transducer probe can be positioned anywhere in the tank so that the displacement of any point of the liquid surface relative to the tank can be monitored.

Tank displacement at lower frequencies was measured with a displacement transducer attached to the flexure arms of the electrodynamic shaker, and at higher frequencies with a Bently transducer positioned to measure the motion of the tank bottom directly. The outputs of both the liquid sur-

face and the tank displacement transducers were monitored simultaneously on a dual trace display of an oscilloscope so that amplitudes of each motion could readily be recorded. In addition, the frequency of the excitation was recorded accurately on an electronic counter.

Basically, two kinds of observations were conducted in the present experiments: mapping stability boundaries, and determining liquid surface responses. Stability boundaries for the $\frac{1}{2}$-subharmonic liquid responses were obtained by fixing excitation frequency at various points in the vicinity of the theoretically predicted boundary for a given mode and then very slowly increasing excitation amplitude at each frequency until the $\frac{1}{2}$-subharmonic motion began to appear. The amplitude increase had to be performed very carefully and slowly to prevent overshooting the stability boundary. Only those parts of boundaries that did not overlap boundaries of other modes could be discerned accurately. Subsequently, an approximate general stability boundary for $\frac{1}{2}$-subharmonic motion was obtained for a frequency range of up to 60 cps, in which, of course, many modes overlapped each other.

Liquid surface responses were obtained for $\frac{1}{2}$-subharmonic, harmonic, and superharmonic liquid motions. These responses were obtained by holding excitation amplitude constant and varying excitation frequency over a narrow band in which a given mode occurred. Here again, in some cases, a substantial amount of time was required before the amplitudes of the motion stabilized to a definite value.

V. Experimental and Theoretical Results for Subharmonic Response

A. Stability Boundaries

Typical results of the experimentally determined stability boundaries for $\frac{1}{2}$-subharmonic motion are shown in Fig. 5 for the $m = 1$, $n = 1$ mode at two different liquid depths, $h/d = 1$ and $h/d = \frac{1}{4}$. The amplitude of the liquid motion, for a tank excitation amplitude and frequency on the right-hand side of the stability boundary, slowly increased as the unstable region was entered; however, on the left-hand side, the amplitude of the liquid motion grew to a considerable magnitude (over a period of several cycles of tank motion)

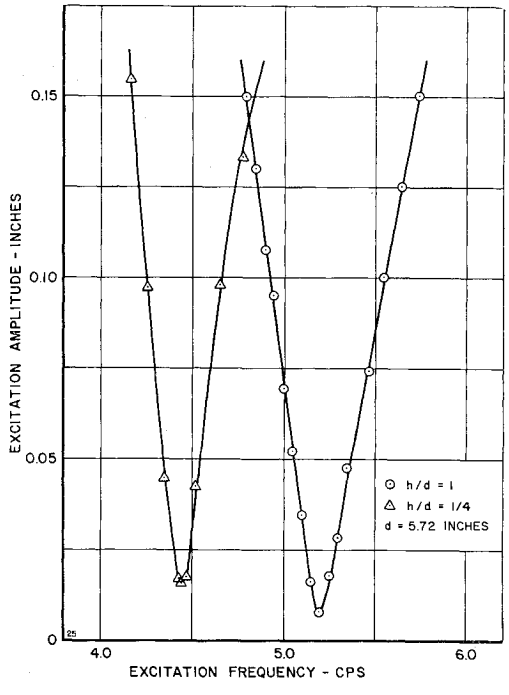

Fig. 5 Experimental stability boundaries for $m = 1$, $n = 1$, $\frac{1}{2}$-subharmonic.

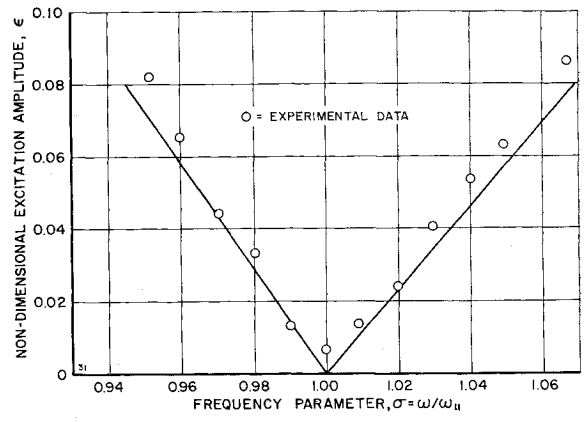

Fig. 6 Theoretical correlation for $m = 1$, $n = 1$, $\frac{1}{2}$-subharmonic stability boundary at $h/d = 1$.

immediately upon entering the unstable region. This behavior, as will be shown later in the discussion, leads to "jump" phenomena.

Figure 5 demonstrates, as discussed previously, that there is a very small amplitude cutoff, probably caused by viscous damping. The resonant frequency of this sloshing mode may be calculated by dividing the tank excitation frequency by two at the point for which the stability boundary most nearly approaches the line $X_0 = 0$. In each case, this frequency was about 2 to 3% larger than the corresponding theoretical natural frequency. The cause of the discrepancy is difficult to explain; it might reflect a lack of exact precision in the frequency measuring apparatus, it might be caused by a slight out-of-roundness of the tank, or it may be due to other causes, such as an apparent shrinkage of the tank diameter because of boundary layers.[17]

Figure 6 compares the stability boundaries given by Eqs. (18) and (19) and the experimental boundaries for the $m = 1$, $n = 1$ mode with $h/d = 1$. A slight decrease in the width of the experimental boundary, probably due to viscous effects, is evident in this figure. It should be pointed out that the experimental values of the frequency parameter σ were nondimensionalized by using the experimental natural frequency. In this way, both the theoretical and experimental curves were forced to begin *at* $\sigma = 1$; however, except as noted previously, it can be seen that the general correlation between theory and experiment is quite good.

Similar experimental stability boundaries for the $m = 0$, $n = 1$ mode at different liquid depths have also been obtained, but are not shown here. Once again, the experimentally determined liquid natural frequency is about 3% higher than the theoretical one. Comparison of the theoretical and experimental boundaries for this mode, as before, shows very good correlation.

B. Liquid Amplitude Response

Figure 7 shows the experimental liquid response in the $m = 1$, $n = 1$ mode, with $h/d = 1$, for three different values of the tank excitation amplitude; a photograph of typical liquid motion for this mode of oscillation is shown in Figure 8. The liquid amplitude plotted in Fig. 7 is one-half the sum of maximum rise and maximum depression of the free surface at the point $\bar{r} = 2.49$ in., $\theta = 0$. The measurements were not taken exactly at the tank wall, which normally would be the point of maximum liquid amplitude in this mode, in order to minimize any effects the wall itself might have on the measuring apparatus and liquid motion.

As the forcing frequency was gradually decreased from a point slightly to the right of the stability boundary (Fig. 5), liquid motion continually increased as the unstable region was traversed, cf. the curve for $X_0 = 0.0860$ in Fig. 8. Once

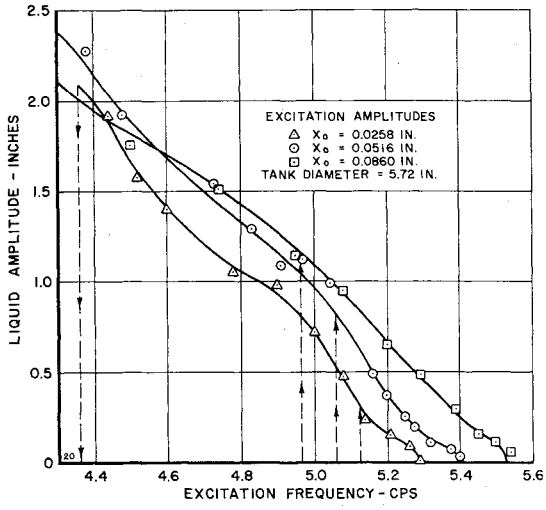

Fig. 7 Experimental liquid response for $m = 1$, $n = 1$, $\frac{1}{2}$-subharmonic at $h/d = 1$.

the liquid motion appeared to reach a steady state, the forcing frequency could be further decreased, even to points considerably to the left of the left-hand stability boundary, i.e., into the stable region for small liquid motions, and the steady-state liquid amplitude would increase still more. However, a point would finally be reached at which the liquid motion quickly decayed to zero, as indicated on Fig. 7 by the downward-pointing dashed arrow on the curve for $X_0 = 0.0258$. For larger excitation amplitudes, the frequency at which the liquid motion ceased was so low that it could not be conveniently shown in the figure. On the other hand, if the frequency were gradually increased from a point to the left of the unstable region (Fig. 5), the liquid surface remained quiescent until the stability boundary was reached. At this point, the liquid amplitude quickly increased to a rather large magnitude, as indicated in Fig. 7 by the upward-pointing dashed arrows in each curve. Both of these types of liquid behavior are similar to the well-known "jump" behavior in other nonlinear dynamic systems.

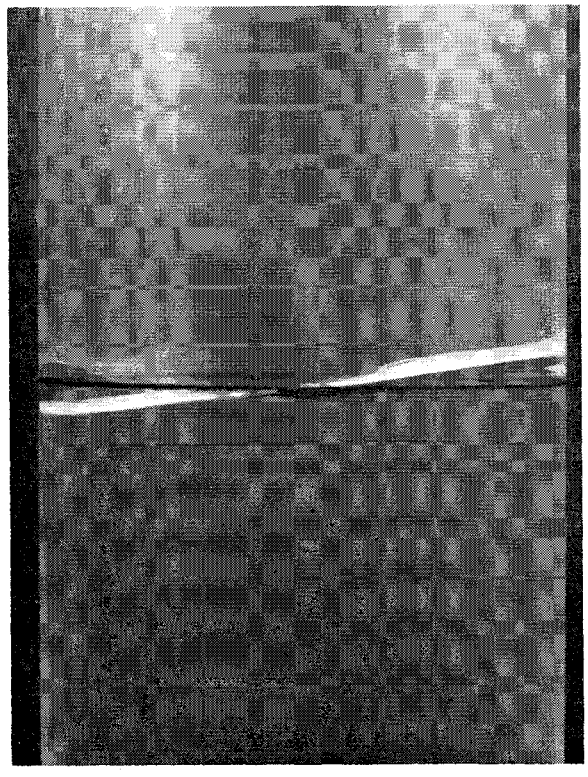

Fig. 8 Typical liquid motion for $m = 1$, $n = 1$, $\frac{1}{2}$-subharmonic.

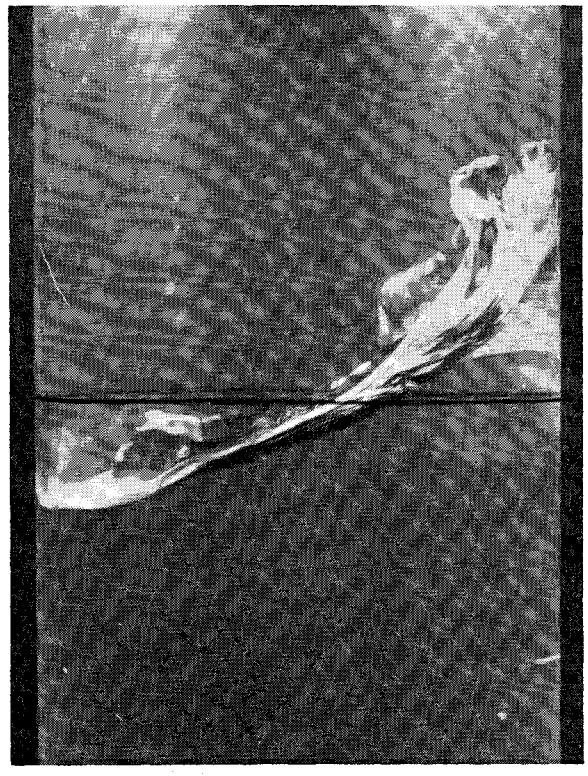

Fig. 9 Large amplitude liquid motion "breaking wave."

The very large amplitude liquid motion, corresponding to the upper part of each curve in Fig. 7, was quite complex. A number of easily observable small liquid motions were superimposed on the basic mode, and in some cases breaking waves were also noticed, as shown in the photograph given in Fig. 9. The response curves have a number of inflection points and "wiggles," and in some instances the curves for different excitation amplitudes actually intersect. Moreover, although the line $\theta = 0$ remained fixed for any given tank excitation frequency and amplitude, its location varied with different excitation frequencies. However, there was no evidence of any time-dependent rotation, periodic or otherwise, of the plane of the liquid motion, as occurs with large-amplitude sloshing resulting from transverse excitation.

The amplitudes of the liquid response for $h/d = \frac{1}{4}$ were generally smaller than those for $h/d = 1$, and the frequency band for which subharmonic motion was possible was also not as wide. For the larger excitation amplitudes, data were not recorded to the point at which the "jump" back to the lower curve occurred because the tank bottom began to interfere with the larger amplitude liquid motion.

Figure 10 shows the theoretical liquid amplitudes, as well as a number of experimental points, for the antisymmetrical mode $m = 1$, $n = 1$, as functions of σ and ϵ. These amplitudes were calculated at the point $\bar{r} = 2.49$ in., $\theta = 0$ by using the equation

$$Y_o = \frac{1}{2}\left[y\left(\frac{\bar{r}}{R} = 0.837, \theta = 0, \sigma t = \frac{\pi}{2}\right) - y\left(\frac{\bar{r}}{R} = 0.837, \theta = 0, \sigma t = \frac{3\pi}{2}\right)\right]$$

where $y(r, \theta, t)$ is given by Eq. (25).

It may be seen from this figure that the comparison between theory and experiment is fairly good for small values of Y_o, but at larger liquid amplitudes the theoretical results deviate severely from the experimental data, chiefly because

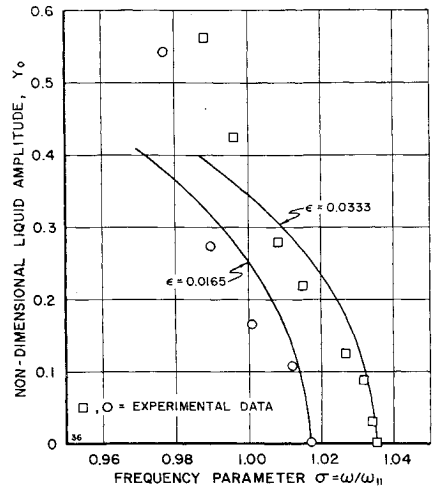

Fig. 10 Theoretical correlation for $m = 1$, $n = 1$, $\frac{1}{2}$-subharmonic liquid response at $h/d = 1$.

the third-order theory used here does not predict the inflection points in the experimental curves, nor the point at which the liquid "jumps" from a very large amplitude to a practically zero amplitude, corresponding to the downward-pointing arrows in Fig. 7.** The upward "jump" from zero to a rather sizable amplitude is, however, predicted.

Figure 11 is a plot of the experimentally determined liquid amplitude at the center of the tank in the $m = 0$, $n = 1$ symmetric mode, for $h/d = 1$; Fig. 12 is a photograph of typical liquid motion for this mode. "Jump" phenomena are once again shown in Fig. 11 by dashed lines. For the largest value of tank excitation amplitude, the symmetric liquid motion was coupled with the $m = 2$, $n = 1$ mode at low excitation frequencies, and with the $m = 3$, $n = 1$ mode at high excitation frequencies. A glance at Fig. 2 shows that such coupling should be expected for these large excitation amplitudes.

Correlation between theory and experiment for the $m = 0$, $n = 1$ symmetrical mode is slightly better than for the

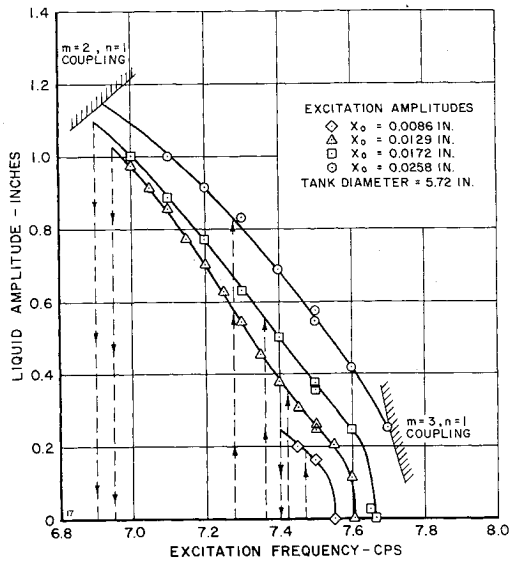

Fig. 11 Experimental liquid response for $m = 0$, $n = 1$, $\frac{1}{2}$-subharmonic at $h/d = 1$.

** In order to predict the downward "jump," it would be necessary to include a dissipation mechanism in the theory, see Ref. 9, pp. 90–94.

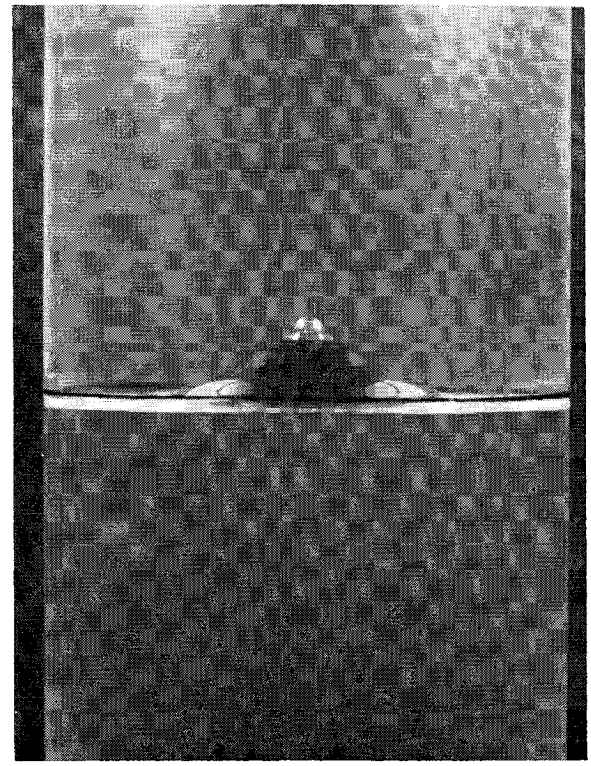

Fig. 12 Typical liquid motion for $m = 0$, $n = 1$, $\frac{1}{2}$-subharmonic.

antisymmetric mode; even so, the theoretical predictions for the large amplitude results are only in qualitative agreement with experiments.

C. Liquid Mode Shapes

Figures 13 and 14 compare experimental and theoretical wave shapes for antisymmetrical and symmetrical liquid motions, each for a given value of σ and ϵ. The wave amplitudes in both figures have been normalized by dividing the amplitude at any point by the maximum amplitude of the wave.

In Fig. 13 the superposition of a symmetrical wave on the basic antisymmetrical $\cos\theta$ wave is clearly evident near $\bar{r}/R = 0$. This part of the wave, as predicted by theory and confirmed by experiment, oscillates at twice the frequency of the predominant wave, i.e., it oscillates at a frequency equal to the forcing frequency. Since the wave shape is nearly the same for both the positive (above $\bar{z} = 0$) and negative (below $\bar{z} = 0$) waves, only the positive wave is shown in Fig. 13. Because of this, the part of the wave to the left of the centerline corresponds to a time one-half cycle later than the part of the wave to the right of the centerline. Correlation between theory and experiment is fairly good.

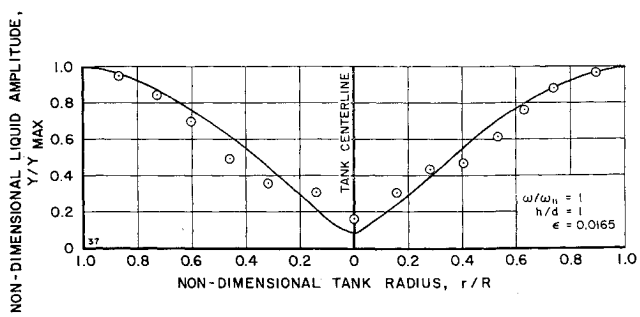

Fig. 13 Comparison of theoretical and experimental wave shapes for $m = 1$, $n = 1$, $\frac{1}{2}$-subharmonic.

Figure 14 shows a symmetrical liquid wave shape. In this case the positive and negative waves are noticeably different, and, therefore, both are shown in the figure. The theoretical and experimental wave shapes, as can be seen, compare very well.

It should be mentioned that the wave shapes shown in Figs. 13 and 14 are quite similar in appearance to the theoretical results of Mack.[18]

VI. Additional Experimental Observations

A. Harmonic and Superharmonic Response

During the course of the experiments, harmonic and superharmonic responses were observed for several different surface modes. These responses, being considerably less prominent than the $\frac{1}{2}$-subharmonic responses, were observed only for excitation amplitude-frequency combinations at which $\frac{1}{2}$-subharmonic motion could not grow from small motions in any mode. For tank excitation frequencies below 8 cps, this, of course, corresponds to all areas outside the $\frac{1}{2}$-subharmonic instability regions shown in Fig. 2.

Experimental data on harmonic response for the $m = 1$, $n = 1$ and $m = 0$, $n = 1$ modes (the period of the liquid motion being the same as that of the excitation) showed that the amplitudes of these liquid responses are small when compared to the amplitude of the $\frac{1}{2}$-subharmonic responses in these modes, for the same excitation amplitude. Nevertheless, these responses were readily measured with the present liquid displacement transducer and, in fact, could easily be seen visually on the liquid surface. The response curves give the appearance of the harmonic forced response of a slightly nonlinear softening, damped system in the vicinity of a resonance. The peaks in these responses occurred essentially at the frequency of the corresponding linear free modes, which, as has already been pointed out, were about 3% higher than the corresponding theoretically predicted frequencies shown in Fig. 2.

It must be recognized that these harmonic and superharmonic responses actually occurred in the vicinity of what are unstable regions for such motions as can be seen, for example, from Fig. 1 for the $m = 1$, $n = 1$ mode. It appeared that the small amplitude harmonic and superharmonic motions observed in the 5.72-in.-diam tank corresponded to *stable* solutions of Mathieu's equation, influenced by the presence of damping. Since the width of the unstable regions increases with decreasing tank diameter, so that amplitude cutoff caused by damping is less pronounced in very small diameter tanks, it was anticipated that these modes could be more easily excited as large amplitude motion in a still smaller tank. Additional observations made in a 3-in.-diam tank showed this to be correct, since both the harmonics and superharmonics of several modes could readily be excited as large amplitude motion in this smaller tank.

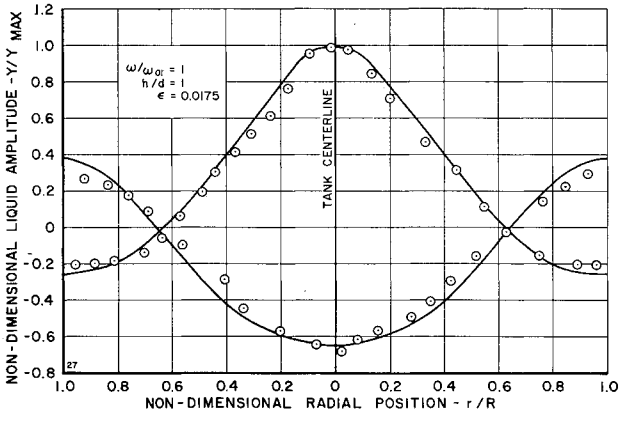

Fig. 14 Comparison of theoretical and experimental wave shapes for $n = 0$, $n = 1$, $\frac{1}{2}$-subharmonic.

B. General Stability Boundary

Because the $\frac{1}{2}$-subharmonic instability regions overlap more and more with increasing frequency, one cannot help but speculate about the effects of damping, as well as about the general behavior of the fluid, throughout a broad range of frequencies encompassing many modes. Figure 15 shows a logarithmic plot of a general $\frac{1}{2}$-subharmonic stability boundary for such a band of frequencies for the 5.72-in.-diam tank. Everywhere above this boundary, $\frac{1}{2}$-subharmonic motion occurs in some mode that depends on the frequency and amplitude of the excitation.†† The first four minima that occur for the lower frequencies are those for the modes shown in Fig. 2. As the excitation frequency is increased, the individual minima become less distinct, because of the increasing overlap of modes, until, above about 20 cps, the boundary becomes nearly a straight line. In addition, higher frequencies require smaller excitation amplitudes to produce $\frac{1}{2}$-subharmonic motion.

Of course, Fig. 15 gives no information about the liquid amplitude once subharmonic motion has begun. An analogous general response curve would be necessary for this purpose. Such a general response curve could be used to describe the resulting liquid behavior as excitation amplitude is increased from zero, at a given frequency. In general, this response might be described as follows: at lower excitation amplitudes the liquid first responds in *stable* harmonic motion in a synchronous mode corresponding to the excitation frequency. Then as the amplitude is increased, the $\frac{1}{2}$-subharmonic stability boundary for some mode is encountered, and a larger amplitude $\frac{1}{2}$-subharmonic liquid motion subsequently results. For example, referring to Fig. 2, near 6.3 eps and for excitation amplitudes less than about 0.03 in., harmonic response in the $m = 0$, $n = 3$ mode occurs; but for a forcing amplitude greater than 0.03 in., subharmonic motion is initiated. As the excitation amplitude is further increased, the liquid motion becomes more and more violent until breaking waves occur. At higher frequencies, corresponding to higher modes, the breaking waves appear as surface spray.

The effects of surface tension become more important for the higher frequency, shorter wavelength modes. Liquid motions in these modes are generally referred to in the literature as capillary waves, but there is no sharp dividing line separating regions where surface tension is important and those where it is not. The subharmonic liquid motion depends entirely on the frequencies of the natural liquid modes, all of which are affected to some extent by surface tension, and the amount of overlap of the unstable regions at the excitation frequency. Referring to the higher frequency modes as capillary waves seems to complicate the description unnecessarily by inferring that these modes are basically different from the lower frequency modes. The results of the present study indicate that this is not the case.

VII. Conclusions

Liquid surface responses to longitudinal excitation exhibit a variety of characteristics, all of which depend principally upon the amplitude and frequency of the tank excitation. In the present paper, only a limited range of frequencies and amplitudes was investigated in order to describe in detail one significant aspect of the general liquid behavior, that is, liquid responses of moderate amplitude in some surface mode of oscillation. As in other types of tank excitation, the lower frequency liquid modes are of most importance for practical applications, except that for longitudinal excitation

†† If there were no damping, the individual minima of this curve would occur at a tank amplitude of zero.

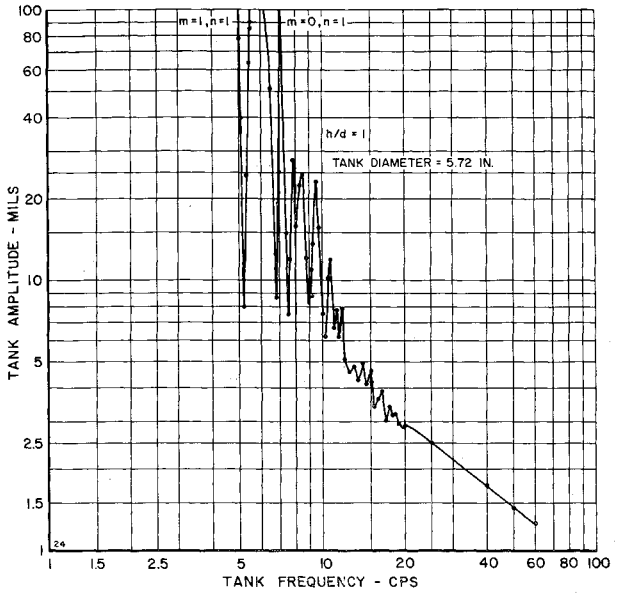

Fig. 15 General $\frac{1}{2}$-subharmonic stability boundary.

the symmetric liquid modes appear as prominently as antisymmetric modes. Liquid surface response in higher frequency modes, often referred to as capillary waves, would appear to have little influence on the over-all vehicle motion unless the amplitude of excitation is so large that violent surface agitation or spray results. This type of response occurs outside the amplitude range considered in the present paper.‡‡

Prediction of regions of one-half subharmonic instability by the Mathieu equation seems to agree very well with experimental data, at least for the cases and ranges of parameters considered here. These analytical predictions would probably constitute valid design criteria for space vehicle propellant tanks, if employed with discretion. Also, the third-order theory presented in this report seems adequate to describe the amplitude and wave shapes of the low-frequency $\frac{1}{2}$-subharmonic motions. More accurate predictions could be obtained by extending the analysis to include fifth- or even higher-order terms; other than the computational effort involved, there does not seem to be any inherent difficulty in such a procedure.

Experimental results indicate that harmonic and superharmonic liquid responses may also occur, although usually with a considerably smaller amplitude than that of the $\frac{1}{2}$-subharmonic response, except in tanks of very small diameter. Such small amplitude responses appear to be an entirely different type of motion than the subharmonic response; in this regard, the absence of "jumps" caused by instabilities in small liquid motions should be noted.§§ A successful theory for these small amplitude harmonic and superharmonic motions has not yet been developed.

Other forms of liquid surface response which occur for excitation ranges outside of those considered in the present report could conceivably be very important for space vehicle considerations. Examples of such responses are: low frequency liquid surface motions generated by high frequency spray phenomena, which occur for much higher oscillatory amplitudes and frequencies[14]; peculiar bubble behavior[15]; and the whole spectrum of liquid interaction with tank motion for the more practical case of an elastic container.[16] These aspects of liquid behavior in a longitudinally oscillated tank require additional study to determine their significance in liquid fuel dynamics in rocket vehicles.

‡‡ Such effects are, however, included within our general program of research and will be reported on separately.

§§ Of course, since the response curves for these motions are slightly nonlinear, jumps would occur for sufficiently large excitation amplitudes. Such jumps, however, are caused by the nonlinearities and not by instabilities in small liquid motions.

Appendix

The constants in Eq. (20) are

$$K_{11} = 0.122515 - \frac{0.045199 - 0.043438\lambda_{01}}{\tanh\lambda_{01}b} + \frac{0.010759\lambda_{11} + 0.09500\lambda_{21}}{\tanh\lambda_{21}b} - \frac{0.149793\lambda_{11}^2}{\lambda_{21}\tanh\lambda_{21}b}$$

$$K_{01} = 0.343624\lambda_{01}\lambda_{11}$$

$$K_{21} = 0.620686\lambda_{11}^2 - 0.044582\lambda_{11}\lambda_{21}$$

$$k_{11} = \frac{0.045199\lambda_{11}^3}{\tanh\lambda_{01}b} + \frac{0.149793\lambda_{11}^4}{\lambda_{21}\tanh\lambda_{21}b} - \frac{0.010759\lambda_{11}^3}{\tanh\lambda_{21}b}$$

$$k_{01} = 0.165118 + \frac{0.171812\lambda_{11}}{\tanh\lambda_{01}b}$$

$$k_{21} = 0.198686 + \frac{0.310343\lambda_{11}^2}{\lambda_{21}\tanh\lambda_{21}b} - \frac{0.02229\lambda_{11}}{\tanh\lambda_{21}b}$$

References

[1] Abramson, H. N., "Dynamic behavior of liquids in moving containers," Appl. Mech. Rev. **16**, 501–506 (1963).

[2] Cooper, R. M., "Dynamics of liquids in moving containers," ARS J. **30**, 725–729 (1960).

[3] Skalak, R. and Yarymovych, M., "Forced large amplitude surface waves," *Proceedings of the Fourth U. S. National Congress on Applied Mechanics* (1962), pp. 1411–1418.

[4] Taylor, G. I., "The instability of liquid surfaces when accelerated in a direction perpendicular to their planes, I.," Proc. Roy. Soc. (London) **A201**, 192–196 (1950).

[5] Bolotin, V. V., "On liquid motion in a vibrating container," Prikl. Mat. Mekhan. **20**, 293–294 (1956).

[6] Benjamin, T. B. and Ursell, F., "The stability of a plane free surface of a liquid in vertical periodic motion," Proc. Roy. Soc. (London) **A225**, 505–515 (1954).

[7] Skalak, R. and Conly, J. F., "Surface waves on a rotating fluid," AIAA J. **2**, 306–312 (1964).

[8] McLachlan, N. W., *Theory and Application of Mathieu Functions* (Oxford University Press, New York, 1951).

[9] Stoker, J. J., *Nonlinear Vibrations* (Interscience Publishers, Inc., New York, 1950).

[10] Abramson, H. N., "Nonlinear vibration," *Shock and Vibration Handbook* (McGraw-Hill Book Co., Inc., New York, 1960).

[11] Penney, W. G. and Price, A. T., "Finite periodic stationary gravity waves in a perfect liquid," Phil. Trans. Roy. Soc. (London) **A244**, 254–284 (1952).

[12] Lamb, H., *Hydrodynamics* (Dover Publications, New York, 1945).

[13] Kana, D. D., Lindholm, U. S., and Abramson, H. N., "An experimental study of liquid instability in a vibrating elastic tank," Southwest Research Institute TR 5, Contract NASw-146, (January 1962).

[14] Yarymovych, M. I., "Forced large amplitude surface waves," D. Sc. Thesis, Columbia Univ. (December 1959).

[15] Dodge, F. T., "A review of research studies on bubble motion in liquids contained in vertically vibrating tanks," Southwest Research Institute TR 1, Contract NAS8-11045 (December 1963).

[16] Kana, D. D., "Longitudinal forced vibration of partially filled tanks," Southwest Research Institute TR 6, Contract NASw-146 (February 1963).

[17] Case, M. M. and Parkinson, W. C., "Damping of surface waves in an incompressible fluid," J. Fluid Mech. **2**, 172–188 (March 1957).

[18] Mack, L. R., "Finite amplitude gravity waves of an ideal liquid in a right circular cylindrical tank with a horizontal bottom," Ph.D. Thesis, Univ. of Michigan (1960).

[19] Dodge, F. T., Kana, D. D., and Abramson, H. N., "Liquid surface oscillations in longitudinally excited rigid cylindrical containers," Southwest Research Institute TR 2, Contract NAS8-11045 (April 1964).